CrossMark

TECHNICAL PAPER

Optimization of a two degrees of freedom compliant mechanism using Taguchi method-based grey relational analysis

Thanh-Phong Dao[1,2] (ID) **· Shyh-Chour Huang[3]**

Abstract This paper presents a multi-response optimal design for new two degrees of freedom compliant mechanism (TDCM) by the use of the hybrid statistical optimization techniques such as Taguchi method, response surface methodology, grey relational analysis and entropy weighting measurement technique. The design parameters like various thicknesses of flexure hinges play a vital role in determining its quality characteristics of TDCM. The quality characteristics of TDCM are assessed by measuring the displacement and first natural frequency. The experimental trials are designed by the Taguchi's L_{25} orthogonal array. A hybrid approach of grey-Taguchi based response surface methodology and entropy measurement is then combined to maximize both the displacement and first natural frequency simultaneously. Response surface methodology is utilized for modeling the relationship between design parameters and two responses with grey relational grade. Entropy measurement technique is employed for calculating the weight corresponding to each of quality characteristics. Analysis of variance (ANOVA) is conducted to determine the significant parameters affecting the responses. ANOVA and confirmation tests are conducted to validate the prediction accuracy and the statistical adequacy of the developed mathematical models. The experimental results
were in a good agreement with the simulation results from ANSYS. The proposed methodology is expected to use for related micropositioning compliant mechanisms.

1 Introduction

TDCM allows two degrees freedom (DOF) motions for ultrahigh precision micropositioning systems. It can be found in wide applications such as biomechanics, ultrahigh machining, micro-electromechanical systems, atomic force microscope, optical fiber alignment, etc. The compliant mechanisms transfers motions based on elastic deformations of the material instead of traditional mechanical joints. Hence, TDCM offers several extra merits, including smooth displacement, no backlash, zero friction, not noise, simplified manufacturing processes, increased precision, increased reliability, and monolithic structure.

In several years, micropositioning compliant mechanisms were widely developed. For example, a compliant micro-positioning platform with embedded strain gauges and viscoelastic damper was designed and analyzed (Dao and Huang 2016). In addition, compliant micropositioning systems with a large range have been developed well for various multi-applications in the book (Xu 2016). The kinematics, statics, stiffness, load capacity, and dynamics for 2-DOF compliant mechanism was modeled using pseudo-rigid-body model (Li and Xu 2011). Besides, a flexure-based micropositioning systems with a large workspace were designed for a variety of precision engineering applications (Xu 2012a, b, c). A new flexure-based dual-stage nanopositioning system was developed for micro-/nanomanipulations (Xu 2012a, b, c). The results of this study achieved a high positioning accuracy, long stroke motion, and high servo bandwidth. A flexure parallel-kinematic

✉ Thanh-Phong Dao
daothanhphong@tdt.edu.vn

1 Division of Computational Mechatronics, Institute for Computational Science, Ton Duc Thang University, Ho Chi Minh City, Vietnam

2 Faculty of Electrical and Electronics Engineering, Ton Duc Thang University, Ho Chi Minh City, Vietnam

3 Department of Mechanical Engineering, National Kaohsiung University of Applied Sciences, 415 Chien-Kung Road, Kaohsiung 80778, Taiwan, ROC

precision positioning stage was designed to obtain a centimeter range and compact dimension (Xu 2014). More recently, a XY flexure nanopositioning stage was developed and controlled (Zhang et al. 2016). A new compliant XY precision positioning stage was designed well with a constant force output (Wang and Xu 2017).

As known, the displacement (DI) and first natural frequency (FR) of TDCM are the most important performances or quality characteristics to affecting the effective performance of ultrahigh precision positioning systems. A broad displacement is suitable for various applications while a high first natural frequency can raise the speed of the mechanism. Some of previous studies only focused on the displacement whereas some concentrated on the first natural frequency. Therefore, this study aims to propose an effective optimization process to improve overall the quality characteristics of the TDCM. The significant contribution of this study is to conduct a statistical-based multi-objective optimization process for TDCM.

For optimization problem based on experiments, the Taguchi method is an efficient tool as it can minimize the number of experiments by using orthogonal arrays. But it fails to multi-objective optimization problem. To simultaneously optimize many quality responses, most researchers suggest a combination of the Taguchi method coupled with others. The Taguchi method can be combined with artificial neural network (ANN), but ANN on the other hand requires voluminous data and tedious training characterized by an uncertainty in finite convergence. Besides, the Taguchi method also integrated with fuzzy logic analysis; however fuzzy logic rules may not be easily amendable to dynamic changes of a process. In order to overcome those approaches, the Taguchi method coupled grey relational analysis (GRA) to optimize multiple quality characteristics is preferred to be used. The reason is that grey relational grade is used as the performance measure in GRA, and the grade values are maximized irrespective of the nature of quality characteristics.

In addition to demonstrate the relationship between the inputs and outputs, the RSM is a more simple statistical regression technique. However, the statistical adequacy must be tested. Hence, ANOVA and statistical criteria are employed to validate the statistical adequacy. Subsequently, prediction accuracy of RSM models is tested by the experimental validation. Another important problem is weighting factor for each quality characteristic. When weighting factor of each response changed, the setting of optimal parameters is also varied. Hence, in multi-objective optimization problem, weighting factor of each response should be determined accurately. The weighting factor can be calculated by the entropy measurement technique. Up to now, the Taguchi method, GRA approach, RSM, and entropy weighting measurement technique have been recognized

as an effective tool; but those methods have still a gap in integration together in order to make a hybrid approach to solve complicated optimal problems. Therefore, the Taguchi method combined with GRA and RSM have been used in the different areas of multi-response optimization involving coating, plasma, drilling, CNC, and so on (Dao 2016; Ilo et al. 2012; Senthilkumar et al. 2014; Muthuramalingam and Mohan 2014; Datta et al. 2009; Kuo et al. 2011; Chiang and Hsieh 2009).

This objective of the paper is to propose a robust multi-response optimal design for the TDCM using a hybrid approach of grey-Taguchi based response surface methodology and entropy weighting measurement technique. The quality characteristics of TDCM are assessed by measuring the first natural frequency and the displacement. The experimental trials are designed by the Taguchi's L_{25} orthogonal array. A hybrid approach of grey-Taguchi based response surface methodology and entropy measurement is then used for multi-response optimization of TDCM. Prior to optimization, RSM is utilized for modeling the relationship between design parameters responses. Entropy measurement technique is employed for calculating the weight corresponding to each of quality characteristics. ANOVA is performed to determine the significant parameters affecting the responses. ANOVA and confirmation tests are applied to validate the prediction accuracy and the statistical adequacy of the developed mathematical models. Lastly, the experiments and simulations are carried out to verify the optimal results.

2 Mechanical design and optimization statement

2.1 Mechanical design

As depicted in Fig. 1, the proposed TDCM includes three main structures: (1) A mobile platform will be connected with four linkages (blue dashed line) through eight leaf springs in a parallelogram configuration (red dashed line parallelogram), (2) each of the four linkages includes four circular hinges and (3) two linkages of circular hinges are connected with a lever amplification mechanism through a leaf spring.

Previous studies, the 2 DOF compliant mechanisms were developed well (Li and Xu 2011; Xu 2014; Zhang et al. 2016; Wang and Xu 2017). In those studies, the rectangular flexure hinges or circular flexure hinges were utilized. However, if the rectangular flexure hinge was only used, the parasitic error would be increased. If the circular flexure hinge was only employed, the displacement of the structure would be limited. Unlike previous studies, in this study, the leaf springs are adopted to enlarge the displacement while circular hinges are selected to achieve a

Fig. 1 A design of the proposed TDCM
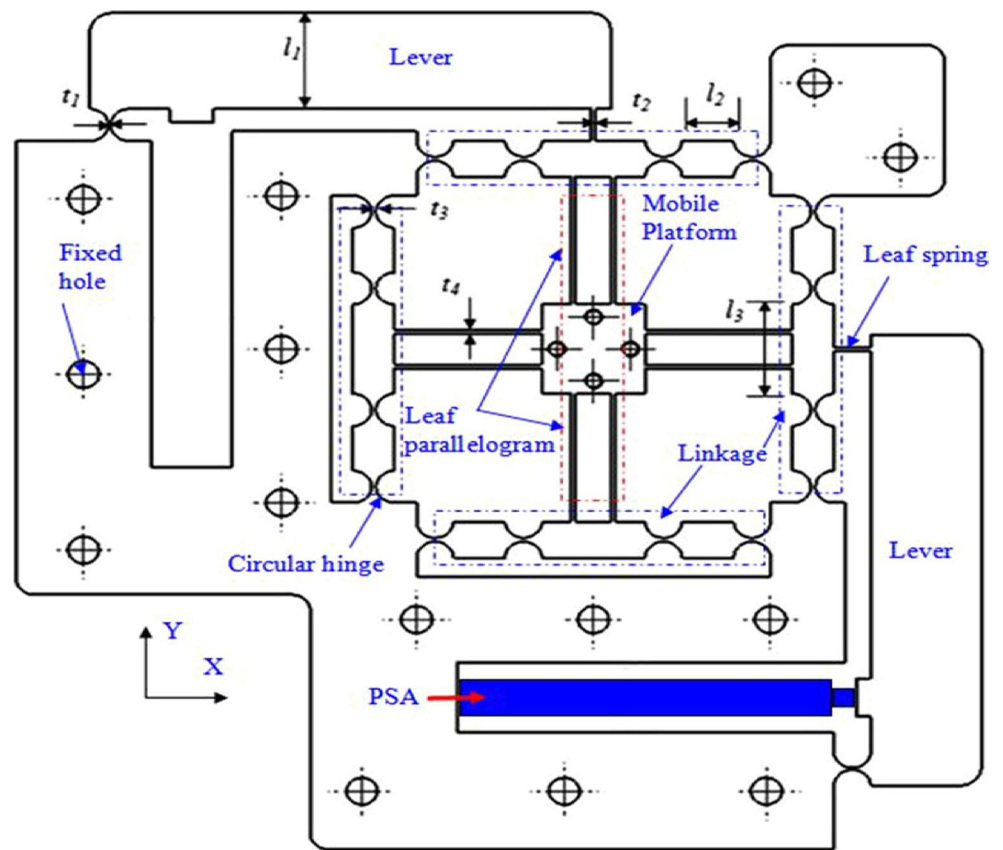
highly accurate center of rotation as an ideal revolute joint to increase the natural frequencies as well as keep the piezo stack actuator (PSA) and lever in good contact.

The ideal design for circular hinges is that when the PSA in the x-axis is activated, the circular hinge of the lever mechanism acts as an ideal rotate joint, and the leaf spring of the lever mechanism initiates a linear motion to the mobile platform through the frame of the circular hinges. At the same time, the leaf springs, which are connected with the mobile platform parallel to the x-axis, transmit the linear motion to the mobile platform due to their high rigidity. In contrast, the leaf springs orthogonal to the x-axis are considered prismatic joints due to their low transverse stiffness. Each frame of circular hinges is arranged in orthogonal structure to gain a good decoupled property or minimum cross-axis coupling. The overall dimensions of the proposed mechanism are 130.9 mm×130.9 mm×8 mm. Compared with previous studies, the dimensions of TDCM has a more compact size. It also has a good decoupling property.

The thickness of flexure hinges is the most important factor affecting the quality characteristics of TDCM. Thus, the design variables consider in further optimization problem as: (1) thickness of circular hinge of lever mechanism t_1, (2) thickness of leaf spring of lever mechanism t_2, (3) thickness of circular hinge t_3 in each linkage, and

(4) thickness of leaf spring t_4 in leaf parallelogram combined with the mobile platform. While the constant values includes: (1) radius of circular hinge: $r = 2.5$ mm, (2) thickness of lever mechanism: $l_1 = 15$ mm, (3) width of elements in each linkage: $l_2 = 7.5$ mm and $l_3 = 14.2$ mm.

The material for the mechanism is chosen as Al 7075-T73 with Young's modulus (E) is 72 GPa, yield strength (σ_y) is 435 MPa. Compared with other materials, this material has a light weight, strong, and has a good fatigue strength.

2.2 Optimization statement

The proposed TDCM is expected to provide a broad displacement and a high first natural frequency. The following multiple-objective optimization problem in this research is briefly described in the standard mathematical format as:

Find: t_1, t_2, t_3, t_4 (1)

Maximize displacement:

$y_1(t_1, t_2, t_3, t_4)$ (2)

Maximize first natural frequency:

$y_2(t_1, t_2, t_3, t_4)$ (3)

Subject to constraints as follows:

$$\sigma = \frac{\sigma_y}{SF} \tag{4}$$

Within ranges:

$$\begin{cases} 0.3\ \text{mm} \leq t_1 \leq 0.7\ \text{mm} \\ 0.3\ \text{mm} \leq t_2 \leq 0.7\ \text{mm} \\ 0.3\ \text{mm} \leq t_3 \leq 0.7\ \text{mm} \\ 0.3\ \text{mm} \leq t_4 \leq 0.7\ \text{mm} \end{cases} \tag{5}$$

where σ_y denotes the yield strength of the adopted material, and $SF \in (1, \infty)$ is the specified safety factor. In this paper, SF is selected as higher than 1.5 because the safety factor is generally selected as large as possible, so that flexible mechanisms can deflect/displacement without failures such as plastic failure or decreased fatigue life. The lower limit of thickness should be at least 0.3 mm for the proposed TDCM fabricated using the wire electrical discharge machining (WEDM) process with a tolerance of ±0.01 mm. The upper limit of the thickness was selected less than or equal 0.7 mm to allow the prototype achieving a large displacement as possible. If it is larger than 0.7 mm, the prototype would be stiffer that leads to the decreased displacement.

Generally, the thickness and radius of flexure hinge is two important factors of a circular flexure hinge (Yong et al. 2008). Hence, they should be considered in the any optimization problems. However, this study would compare the sensitivity of thickness with that of the radius of the circular flexure hinge to investigate the effect of the main
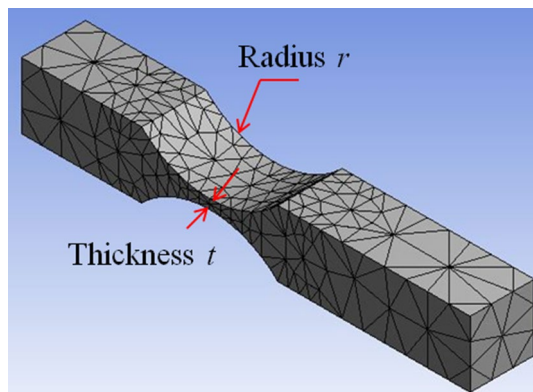
parameters. A model of the circular flexure hinge was as depicted in Fig. 2. The thickness t and radius r were varied to construct 7 models as ($t = 0.3$ mm and $r = 1.2$ mm; $t = 0.4$ mm and $r = 1.4$ mm; $t = 0.45$ mm and $r = 1.6$ mm; $t = 0.5$ mm and $r = 1.8$ mm; $t = 0.55$ mm and $r = 2.0$ mm, $t = 0.6$ mm and $r = 2.2$ mm; $t = 0.7$ mm and $r = 2.5$ mm). Finite element method in ANSYS was utilized to analyze the flexure hinge. The results of displacement and first natural frequency were collected, and then the results were analyzed using ANOVA. The results of ANOVA showed that the thickness of the flexure hinge is the most significant parameter with a value of F-test of 1.5, and followed by the radius of the flexure hinge with a value of F-test of 1.1, as given in Table 1. Hence, the thickness was chosen as the key design variable and the radius of flexure hinge was ignored in the multi-objective optimization of TDCM.

3 Methodology

In general optimization process, mathematical models are formulated firstly, and then an optimal algorithm is applied. However, if modeling errors from mathematical models become large, optimal results will be unacceptable. From that point of view, this study is based on a number of experiments to establish an optimization process without modeling errors. A hybrid approach of grey-Taguchi based response surface methodology and entropy measurement technique is adopted as an effective optimization tool for the proposed TDCM.

Figure 3 shows a systematic flowchart for the multi-objective optimization procedure using a hybrid approach of grey-Taguchi based response surface methodology and entropy measurement technique. The optimization process is divided into key steps as follows:

Step 1   *Define problem*
Step 2   *Define control factors and quality characteristics*
Step 3   *Design of experiments using the orthogonal array of the Taguchi method*
Step 4   *Experimental data collection*
Step 5   *Determine the effect of the control factors on the quality characteristics.*

Fig. 2 Model of circular flexure hinge

Table 1 Controlling factors and their levels

Design variable	Coded	levels				
		Level 1	Level 2	Level 3	Level 4	Level 5
t_1 (mm)	A	0.3	0.4	0.5	0.6	0.7
t_2 (mm)	B	0.3	0.4	0.5	0.6	0.7
t_3 (mm)	C	0.3	0.4	0.5	0.6	0.7
t_4 (mm)	D	0.3	0.4	0.5	0.6	0.7

Fig. 3 The flowchart of multi-response optimal design approach
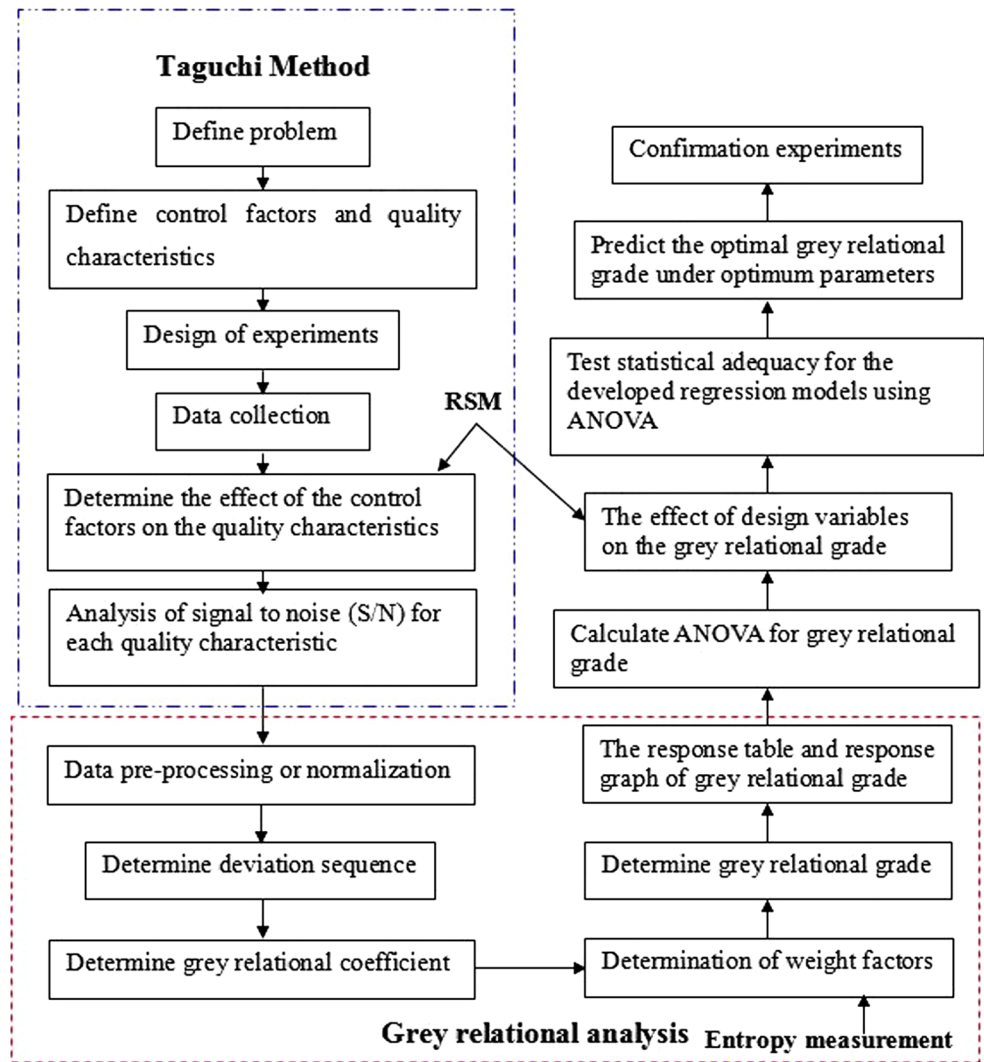
Response surface methodology (RSM) is used to describe this relationship. This relationship is investigated by a quadratic polynomial regression model. A quadratic polynomial regression model is the most popular due to its flexibility to an approximate nonlinear response, and the mathematical model of the quadratic regression model is described below because first-order models often give lack-of-fit (Sharma and Yadava 2012).

$$y = \beta_0 + \sum_{u=1}^{N} \beta_u x_u + \sum_{u=1}^{N} \beta_{uu} x_u^2 + \sum_u \sum_v \beta_{uv} x_u x_v + \varepsilon \quad (6)$$

where y is the predicted output parameter, x is the design variable, N is the number of design variables, β_u ($u = 0, 1, 2,..., N$) are regression coefficients, β_{uu} and β_{uv} are quadratic coefficients. These regression coefficients can be determined by least square method (Montgomery 1997). ε is the model error which is neglected because the

computational optimization are carried out at constant temperature and ignored geometric errors.

Step 6 *Analysis of signal to noise (S/N) for each quality characteristic*

Calculate the *S/N* ratio (η) for various observed responses using the Taguchi method. The higher the better is chosen for two responses (including displacement and first natural frequency) in this study, which described as follows:

$$S/N(\eta) = -10 \log \left(\frac{1}{r} \sum_{k=1}^{r} \left(\frac{1}{y_i^2} \right)_k \right) \quad (7)$$

where y_i is the observed response value of ith experiment. r is the number of experimental repetitions of y_i, ($i = 1, 2,..., n$; $k = 1, 2, ..., m$. n is the number of experiments and m is the number of responses.

Step 7   *Data pre-processing or normalization* Data pre-processing is a transferring the original sequence to become a comparable sequence. The *S/N* ratio of each response is then normalized as $z_i(k)$ ($0 \leq z_i(k) \leq 1$) through the below to avoid the effect of adopting different units and reduce the variability.

Calculate the normalized *S/N* ratio $z_i(k)$ values for n experiments to adjust the values measured on different scales to a common scale. The normalized values of the *S/N* ratio vary between o and 1. The higher the better is used for both responses.

$$z_i(k) = \frac{\eta_i(k) - \min\eta_i(k)}{\max\eta_i(k) - \min\eta_i(k)} \tag{8}$$

where $z_i(k)$ is the normalized *S/N* value for the kth response ($k = 1, 2, \ldots, m$) in the ith experiment (known as the comparability sequence of *S/N* data), $\eta_i(k)$ indicates the estimated *S/N* value (known as the original sequence of *S/N* ratio data). max η_i and min η_i are the largest and smallest values of η_i, respectively. η_i is the ith *S/N* ratio value.

Step 8   *Determine deviation sequence*

$$\Delta_{0i}(k) = \|z_0(k) - z_i(k)\| \tag{9}$$

where $\Delta_{0i}(k)$ is the absolute difference between $z_0(k)$ and $z_i(k)$. $z_0(k)$ presents the ideal value (optimal value; generally equals to 1 in a normalized sequence) for the kth response.

Step 9   *Determine grey relational coefficient* The grey relational coefficient expresses the relationship between the best and actual normalized *S/N* ratio. The grey relational coefficient can be computed as follows.

$$\gamma_i(k) = \frac{\Delta_{\min} + \delta\Delta_{\max}}{\Delta_{0i}(k) + \delta\Delta_{\max}} \tag{10}$$

where $\Delta_{\min}$ is the smallest value of Δ_{0i}, $\Delta_{\max}$ is the largest value of Δ_{0i}, and δ is the distinguishing coefficient $0 \leq \delta \leq 1$ for adjusting the interval of $\gamma_i(k)$. δ is set as 0.5 for average distribution and due to the moderate distinguishing effects and good stability of outcomes. Hence, δ is set as 0.5 for further analysis in the current work.

Step 10   *Determination of weight factors* The mapping function f_i:[0, 1] → [0, 1] subjected to the three conditions as follows (Wen et al. 1998):

$$f_i(0) = 0 \tag{11}$$

$$f_i(x) = f_i(1 - x) \tag{12}$$

where $f_i(x)$ is the monotonic increasing in the range of $x \in (0, 0.5)$.

Hence to define the mapping function for entropy measure to be defined as follows:

$$w_e(x) = xe^{(1-x)} + (1 - x)e^x - 1 \tag{13}$$

This function achieves the maximum value when $x = 0.5$ and the value is as follows:

$$w_e(0.5) = e^{0.5} - 1 = 0.6487.$$

To get the mapping result in the range [0, 1], a new entropy is defined as follows (Wen et al. 1998):

$$W \equiv \frac{1}{(e^{0.5} - 1)} \sum_{i=1}^{n} w_e(x_i) \tag{14}$$

The following steps are used for calculating weight of each response.

Sum of the grey relational coefficient in all sequences of each quality characteristic is as:

$$D_k = \sum_{i=1}^{n} \gamma_i(k), \quad k = 1, \ldots m \tag{15}$$

Entropy of each response is as follows:

$$e_k = K \sum_{i=1}^{n} w_e\left(\frac{\gamma_i(k)}{D_k}\right) \tag{16}$$

where $K = \frac{1}{(e^{0.5}-1) \times n} = \frac{1}{0.6487 \times n}$ is the normalized coefficient.

Sum of entropy is as follows:

$$E = \sum_{k=1}^{m} e_k \tag{17}$$

Normalized weight of each response is calculated as follows:

$$w_k = \frac{1}{m - E} \times \frac{1 - e_k}{\sum_{k=1}^{m} \frac{1}{m-E}(1 - e_k)} \tag{18}$$

where $\lambda_k = \frac{1-e_k}{m-E}$ is the relative weighting coefficient.

Step 11   *Determine grey relational grade* Compute the grey relational grade (*GRG*) by finding the mean of the grey relational coefficient values. The grey relational grade values are taken as the single representatives for multiple responses. The grey relational grade reflects the degree of influence between the comparability sequence and reference sequence. If the grey relational grade equals to unity; it implies the sequences are identical

and all are having values equal to unity. A high grey relational grade corresponds to brawny relational degree between original sequence and reference sequence and yields the factor combinations closer to optimal setting. Mathematically grey relational grade is expressed as follows:

$$\psi_i = \frac{1}{m} \sum_{k=1}^{m} \gamma_i(k). \tag{19}$$

However, the relative significance of the responses varies as per requirement. In practice, all responses are having unequal weights which leads to modification of the above equation, as in cited in, is expressed as.

$$\psi_i = \sum_{k=1}^{m} w_k \gamma_i(k) \tag{20}$$

where $\sum_{k=1}^{m} w_k = 1$. w_k denotes for weight factor for kth quality characteristic. Total of weights is equal to one.

Step 12 *The response table and response graph of grey relational grade* Determine the optimal parameters based on the response table and response graph of grey relational grade though the Taguchi method.

Step 13 *Calculate ANOVA for grey relational grade* Analysis of variance (ANOVA) is used to estimate the significant contribution of each factor on the grey relational grade.

Step 14 *The effect of design variables on the grey relational grade* Response surface methodology is used to describe the relationship between design variables and the grey relational grade. From that, it can determine effect of design variables on the grey relational grade using Eq. (1).

Step 15 *Test statistical adequacy for the developed regression models using* ANOVA Analysis of variance (ANOVA) is used to test statistical adequacy for the developed regression models.

Step 16 *Predict the optimal grey relational grade under optimum parameters* The optimal grey relational grade is predicted considering the effect of all parameter or the most significant parameter. The estimated mean of the grey relational grade can be determined as.

$$\mu_G = G_m + \sum_{s=1}^{q} (G_0 - G_m) \tag{21}$$

where μ_G is the optimal *GRG* value of predicted mean, G_m is the total mean of grey relational grade, G_0 is the optimal mean grey relational grade for each level of factor, q is the number of significant parameters affecting on the grey relational grade.

In order to judge the closeness of the observed value with the predicted value, the confidence interval (*CI*) value of the predicted value for the optimum factor level combination is determined. The 95% confidence interval of confirmation experiments (*CI*) is calculated using the following expression (Dao and Huang 2015):

$$CI_{CE} = \pm \sqrt{F_\alpha(1, fe) Ve \left(\frac{1}{n_{eff}} + \frac{1}{R_e} \right)} \tag{22}$$

where $\alpha = \text{risk} = 0.05$; $F_\alpha(1, fe) = F_{0.05}(1, fe)$ is the F-ratio at 95% $(1 - \alpha)$ confidence interval against degrees of freedom 1 and degrees of freedom of error f_e (Montgomery 1997); V_e is the variance of error (get from ANOVA), $n_{eff} = n/(1 + d)$; N is the total trial number in the orthogonal array; d is the total degrees of freedom of factors associated in estimates of the mean μ, and R_e is the number of repetitions for the confirmation experiment.

Step 17 *Confirmation experiments* The confirmation experimentations are carried out to test the prediction accuracy of developed regression model and validate the optimal results.

4 Results and discussion

4.1 Experimental plan

This study discusses the relationship between the design variables and quality characteristics of TDCM, in order to determine the optimized combination of design variables. First, the composition of various factors and level values are designed based on the Taguchi method, as given in Table 1.

TDCM has two important quality characteristics, namely displacement and first natural frequency. As TDCM requires a broad displacement and a high first natural frequency, this study selects the larger-the-better for two responses according to the Taguchi method. With four process parameters and five levels, the experimental plan was designed via using the orthogonal array L_{25} of the Taguchi method, as shown in Table 2. The 25 experimental tests were conducted to collect the data of the displacement and first natural frequency. The experimental equipments were installed on a vibration isolated optical table (DAEIL systems, Model: DVIO-I-1209M-100t, Korea) to avoid any unexpected vibrations. The prototypes were fabricated via using wire electrical discharge machining.

Table 2 Design of experiments

No. trial	t_1	t_2	t_3	t_4
1	0.3	0.3	0.3	0.3
2	0.3	0.4	0.4	0.4
3	0.3	0.5	0.5	0.5
4	0.3	0.6	0.6	0.6
5	0.3	0.7	0.7	0.7
6	0.4	0.3	0.4	0.5
7	0.4	0.4	0.5	0.6
8	0.4	0.5	0.6	0.7
9	0.4	0.6	0.7	0.3
10	0.4	0.7	0.3	0.4
11	0.5	0.3	0.5	0.7
12	0.5	0.4	0.6	0.3
13	0.5	0.5	0.7	0.4
14	0.5	0.6	0.3	0.5
15	0.5	0.7	0.4	0.6
16	0.6	0.3	0.6	0.4
17	0.6	0.4	0.7	0.5
18	0.6	0.5	0.3	0.6
19	0.6	0.6	0.4	0.7
20	0.6	0.7	0.5	0.3
21	0.7	0.3	0.7	0.6
22	0.7	0.4	0.3	0.7
23	0.7	0.5	0.4	0.3
24	0.7	0.6	0.5	0.4
25	0.7	0.7	0.6	0.5

A high speed bipolar amplifier (Model HAS 4011) from NF Corporation is utilized to drive the PSA (Model 150/5/40 VS10) from Piezomechanik GmbH. Retro-reflective tape from ONO SOKKI Company is attached at the top of each thin aluminum beam; this aluminum leaf is then fixed onto the mobile platform using screws. A preload is applied on the PSA. A laser vibrometer sensor (Model LV-170) the ONO SOKKI Company with high resolution in nano-scale is used to measure the displacement. A frequency response analyzer (Model FRA 5097) from the NF Corporation is used. Frequency response analyzer display software is installed in the computer. Using the FRA display software, the data are displayed on diagrams. Overall experiments are repeated four times. The experimental set-up of displacement is shown in Fig. 4.

The measurements of the first natural frequency within the range of 500 Hz to 5 kHz are performed to evaluate the dynamic characteristics of the mechanism. A modal hammer (Model 9722A2000-SN 2116555) from KISTLER is used to apply the excitation to the mechanism, and the frequency response is measured by using an
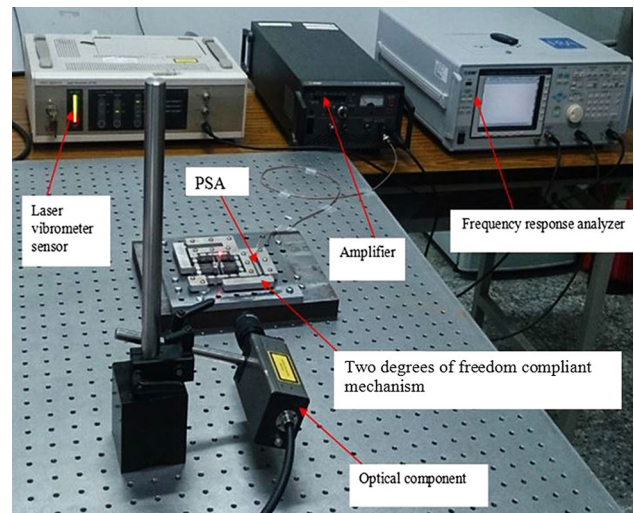
Fig. 4 Experimental measurement of displacement response
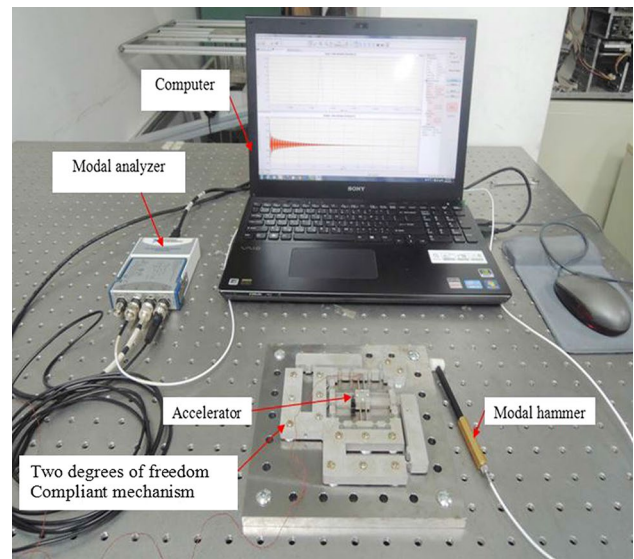
Fig. 5 Experimental measurement of frequency response

accelerator (Model 4744892) from KISTLER. The accelerator is attached to be opposite the excitation from the modal hammer. A modal analyzer (Model NI USB 9162) from National Instruments is utilized in data acquisition and analysis. At the end of the hammer, a force sensor is attached to measure the applied force from the hammer. CUTPRO software is installed in a computer to analyze the data. The experimental set-up of first natural frequency is presented in Fig. 5. The experiments are repeated five times. The first natural frequency is measured for the x-axis. The experimental data and signal to noise ratios of two responses are collected in Table 3.

Table 3 Experimental average results and *S/N* ratios of two responses

No. trial	y_1 (mm)	S/N of y_1	y_2 (Hz)	S/N of y_2
1	0.167	−15.5457	902.597	59.1099
2	0.144	−16.8328	901.613	59.1004
3	0.124	−18.1316	899.299	59.0781
4	0.106	−19.4939	895.655	59.0428
5	0.091	−20.8192	890.681	58.9944
6	0.133	−17.5230	904.039	59.1237
7	0.110	−19.1721	902.788	59.1117
8	0.091	−20.8192	900.207	59.0868
9	0.089	−21.0122	912.376	59.2035
10	0.138	−17.2024	896.746	59.0534
11	0.100	−20.0000	913.233	59.2116
12	0.096	−20.3546	901.035	59.0948
13	0.082	−21.7237	898.747	59.0727
14	0.124	−18.1316	896.451	59.0505
15	0.111	−19.0935	893.050	59.0175
16	0.094	−20.5374	893.299	59.0199
17	0.078	−22.1581	892.074	59.0080
18	0.114	−18.8619	903.111	59.1148
19	0.099	−20.0873	900.774	59.0923
20	0.099	−20.0873	912.394	59.2036
21	0.077	−22.2702	892.358	59.0108
22	0.107	−19.4123	916.728	59.2448
23	0.105	−19.5762	903.981	59.1232
24	0.095	−20.4455	901.937	59.1035
25	0.088	−21.1103	898.562	59.0710

4.2 Effect of design variables on quality characteristics

Prior to an optimization problem, an investigation on the effects of controlling parameters on quality characteristics is necessary actually. A quadratic model, second-order polynomial equation, is developed to explain the effects of parameters on the quality characteristics of TDCM.

The RSM methodology, an interaction between the statistics and mathematics is used to illustrate this relationship. After eliminating the insignificant terms ('Prob > F' larger than 0.05) of parameters, the final mathematic models for displacement and frequency are precise achieved. The mathematic models were developed based on the collected data from 25 experiments and could predict the results of each response at discrete values.

The mathematic model of displacement is derived as follows.

$$y_1 = 0.32948 - 0.15272t_1 - 0.07219t_2 - 0.47825t_3 \\ - 0.18693t_1t_2 + 0.44399t_1t_3 + 0.30044t_2t_3 \quad (23)$$

The mathematic model of first natural frequency is derived as follows.

$$y_2 = 177.833t_1t_2 - 325.054t_1t_3 + 173.873t_1t_4 - 226.113t_2t_4 \quad (24)$$

Three-dimensional plots (response surface) illustrate the effects of design variables on the displacement and first natural frequency, which were drawn based on the mathematic models. As visualized from Fig. 6, it is observed that the displacement lowers rapidly with a decrease in thickness t_1 (about 0.35 mm). Then it decreases gradually with an increase in thickness t_1 (about 0.5 mm). Lastly, it gradually increases with an increase in thickness t_1 (up to 0.7 mm). The displacement significantly increases with an increase in thickness t_2 (about 0.35 mm), and then gradually decreases with in thickness t_2 (up to 0.7 mm). It means that the displacement varies in a curvilinear manner with a change in thicknesses t_1, t_2. As seen in Fig. 7, the displacement sharply decreases with an increase in thickness t_3 (about 0.35 mm), then varies and decreases gradually to thickness t_3 (about 0.7 mm). The displacement first varies in most of periodic manner with an increase in thickness
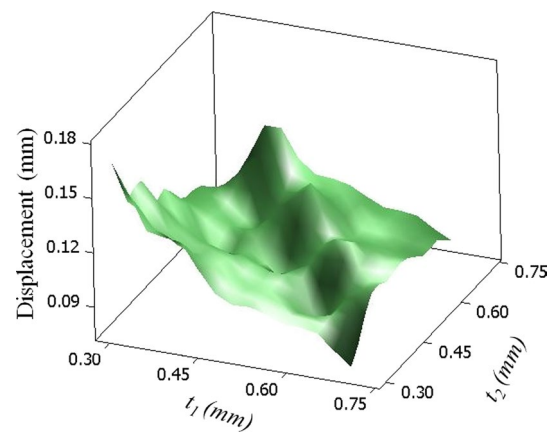
Fig. 6 Surface plot of displacement versus t_1 and t_2
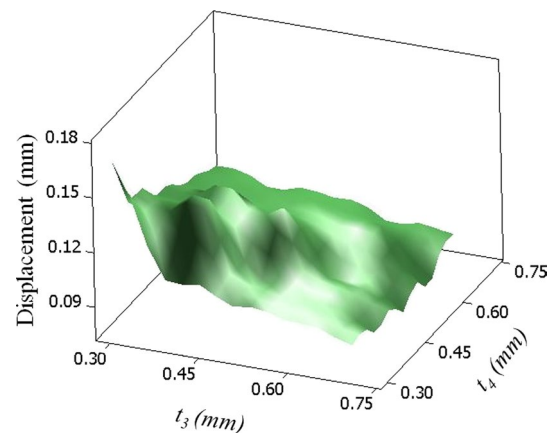
Fig. 7 Surface plot of displacement versus t_3 and t_4
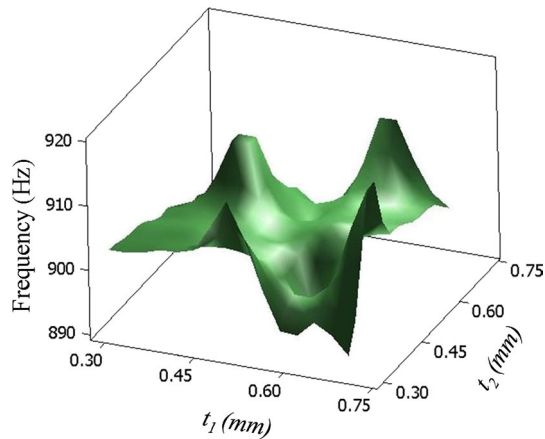
Fig. 8 Surface plot of frequency versus t_2 and t_1

Fig. 9 Surface plot of frequency versus t_3 and t_4

t_4 (from 0.3 mm to 0.6 mm), then increases quickly with an increase of thickness t_4 (from 0.6 mm to 0.7 mm). The results concluded that the thicknesses t_1, t_2, t_3, and t_4 are significantly affecting on the displacement. As a result, these parameters would be optimized to maximize displacement for TDCM. The results also showed that the maximum value of displacement is obtained at the minimum level of t_1, t_2, t_3, and t_4 (0.3 mm). This is due to the fact that the smaller thickness of flexure hinges, the larger displacement is. The maximum displacement is most desirable for any 2-DOF compliant mechanisms.

As depicted in Fig. 8, the first natural frequency first gradually increases with an increase in thickness t_1 from 0.3 to 0.45 mm, and then rapidly rises corresponding to the value of t_1 of 0.5 mm. Lastly, it sharply decreases corresponding to the value of t_1 of 0.6 mm, and then gradually reduces with an increase in thickness t_1 from 0.6 to 0.7 mm. The first natural frequency sharply increases with an increase in thickness t_1 from 0.3 to 0.45 mm, and then gradually decreases corresponding to the value of t_1 from 0.45 to 0.7 mm. It is implied that the first natural frequency varies in a non-linear profile with a change in thicknesses of t_1 and t_2. As seen in Fig. 9, the first natural frequency first gradually increases with an increase in thickness t_3 from 0.3 to 0.45 mm, and then rapidly decreases corresponding to the value of t_3 of 0.5 mm. Lastly, it sharply increases corresponding to the value of t_3 of 0.6 mm, and then gradually increases with an increase in thickness t_4 from 0.6 to 0.7 mm. The first natural frequency gradually varies with an increase in thickness t_1 from 0.3 to 0.7 mm. It is revealed that the first natural frequency varies in a non-linear profile with a change in thicknesses of t_3 and t_4. Hence, these parameters would be optimized to maximize first natural frequency for TDCM. From Fig. 8, the maximum value of first natural frequency is achieved at the maximum level of t_1 (0.7 mm) and minimum level of t_2 (0.3 mm). As depicted
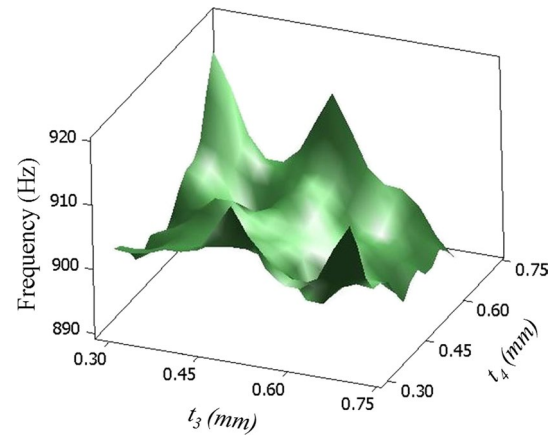
in Fig. 9, the maximum value of first natural frequency is achieved at the minimum level of t_3 (0.3 mm) and maximum level of t_4 (0.7 mm). It is due to the fact that the thickness of flexure hinges is increased, the stiffness of TDCM is also raised. This leads to the increased first natural frequency. A high first natural frequency is most desirable for any 2-DOF compliant mechanisms.

From the discussion above, four design variables were all effecting on two quality characteristics. However, the maximum value of displacement conflicts with the maximum value of first natural frequency corresponding to the design variables. So, this study is aimed to find the optimal combination of processing parameters to maximize displacement and first natural frequency simultaneously.

4.3 Multi-response optimization

After calculating *S/N* ratios for each response, the normalized *S/N* values are subsequently computed. The deviation sequence, the grey relational coefficient, the weight factor of each response, and the grey relational grade are determined. Lastly, the response table and response graph of grey relational grade are illustrated based on the Taguchi method to achieve the optimal parameters. The achieved weight factor was substituted into the grey relational analysis to obtain the grey generation data of each sequence.

The normalized weight factor of displacement and first natural frequency was calculated based on the entropy measurement technique. The weight factor of displacement is 0.5 and first natural frequency was 0.5. The difference sequences, grey relational coefficient, and grey relational grade are shown in Table 4. From Eqs. (9) to (20), k in bracket (k) represents various responses. The displacement response is corresponding to $k = 1$ while the frequency response is corresponding to $k = 2$. For example, z_i (1) is the normalized *S/N* of displacement and z_i (2) is the

Table 4 Grey generation data of each sequence, difference sequence, grey relational coefficient, grey relational grade, and rank of grey relational grade

No.	$z_i(1)$	$z_i(2)$	$\Delta_{0i}(1)$	$\Delta_{0i}(2)$	$\gamma_i(1)$	$\gamma_i(2)$	ψ_i	Rank
1	1.0000	0.4611	0.0000	0.5389	1.0000	0.4813	0.7406	1
2	0.8086	0.4232	0.1914	0.5768	0.7232	0.4643	0.5938	4
3	0.6155	0.3341	0.3845	0.6659	0.5653	0.4288	0.4971	9
4	0.4129	0.1932	0.5871	0.8068	0.4599	0.3826	0.4213	17
5	0.2158	0.0000	0.7842	1.0000	0.3893	0.3333	0.3613	23
6	0.7060	0.5164	0.2940	0.4836	0.6297	0.5084	0.5690	6
7	0.4607	0.4684	0.5393	0.5316	0.4811	0.4847	0.4829	11
8	0.2158	0.3691	0.7842	0.6309	0.3893	0.4421	0.4157	19
9	0.1871	0.8349	0.8129	0.1651	0.3808	0.7518	0.5663	7
10	0.7536	0.2354	0.2464	0.7646	0.6699	0.3954	0.5326	8
11	0.3376	0.8675	0.6624	0.1325	0.4301	0.7905	0.6103	3
12	0.2849	0.4010	0.7151	0.5990	0.4115	0.4549	0.4332	16
13	0.0813	0.3128	0.9187	0.6872	0.3524	0.4211	0.3868	22
14	0.6155	0.2240	0.3845	0.7760	0.5653	0.3919	0.4786	13
15	0.4724	0.0922	0.5276	0.9078	0.4866	0.3552	0.4209	18
16	0.2577	0.1018	0.7423	0.8982	0.4025	0.3576	0.3800	21
17	0.0167	0.0542	0.9833	0.9458	0.3371	0.3458	0.3415	24
18	0.5068	0.4808	0.4932	0.5192	0.5034	0.4906	0.4970	10
19	0.3246	0.3909	0.6754	0.6091	0.4254	0.4508	0.4381	15
20	0.3246	0.8356	0.6754	0.1644	0.4254	0.7526	0.5890	5
21	0.0000	0.0653	1.0000	0.9347	0.3333	0.3485	0.3409	25
22	0.4250	1.0000	0.5750	0.0000	0.4651	1.0000	0.7326	2
23	0.4006	0.5142	0.5994	0.4858	0.4548	0.5072	0.4810	12
24	0.2713	0.4357	0.7287	0.5643	0.4069	0.4698	0.4384	14
25	0.1725	0.3056	0.8275	0.6944	0.3766	0.4186	0.3976	20

Fig. 10 Plot of GRG values for various experiments
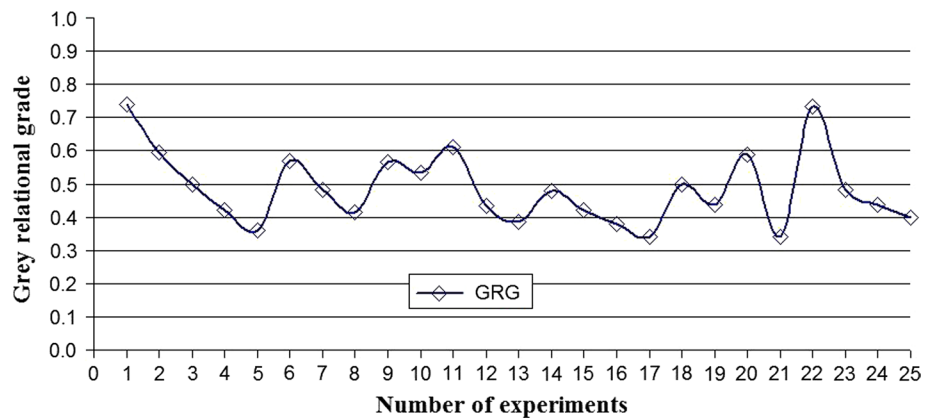
normalized *S/N* of frequency. $\Delta_{0i}(1)$ and $\Delta_{0i}(2)$ are deviation sequences of displacement and frequency, respectively. $\gamma_i(1)$ and $\gamma_i(2)$ are grey relational coefficients of deviation sequences of displacement and frequency, respectively. In Table 4, Δ_{min} is equal to zero (the smallest value of Δ_{0i}), Δ_{max} is equal to one (the largest value of Δ_{0i}).

The highest grey relational grade in the sequence indicates the closest value to the desired value of the quality responses. Therefore, this study was drawn a plot of grey relational grade value corresponding to each experiment, as

depicted in Fig. 10. It is clear observed from Table 4 and Fig. 10 that the maximum value of GRG is observed at the 1st experiment, which indicates that the optimal setting of parameters is close to the parameters combination of the 1st experiment.

The average grey relational grade for each input parameter level was calculated in Table 5. The response graph for average grey relational grade at parameter level was plotted as in Fig. 10. Based on the Taguchi method, the results from Table 5 and Fig. 11 indicated that the optimal input parameter

Table 5 Response table for the average *GRG* for each parameter level

Factor	Mean of *GRG* for each level of each parameter					Max–min	Rank
	Level 1	Level 2	Level 3	Level 4	Level 5		
A	0.5228	0.5133	0.4660	0.4491	0.4781	0.0737	3
B	0.5282	0.5168	0.4555	0.4685	0.4603	0.0726	4
C	0.5963	0.5006	0.5235	0.4096	0.3994	0.1969	1
D	0.5620	0.4663	0.4568	0.4326	0.5116	0.1294	2

Total mean value of *GRG* is 0.4859
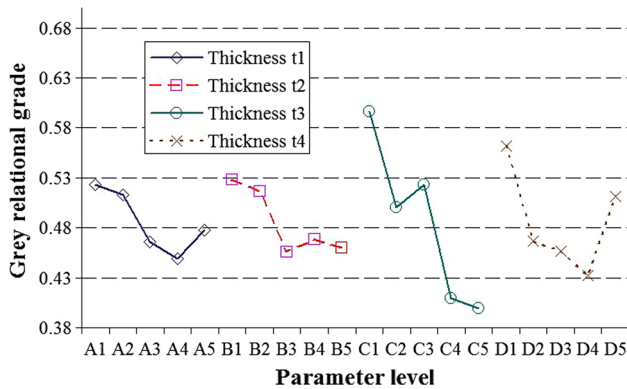
Fig. 11 Response graph of grey relational grade

level is A1B1C1D1 corresponding to thickness t_1 at level 1 (0.3 mm), thickness t_2 at level 1 (0.3 mm), thickness t_3 at level 1 (0.3 mm), and thickness t_4 at level 1 (0.3 mm), which is also the 1st experiment. The results showed that the maximum displacement is equal to 0.167 mm and the maximum first natural frequency is equal to 902.597 Hz.

4.4 ANOVA for grey relational grade

ANOVA was computed to understand the influence of design parameters on the quality characteristics. Table 6 shows that factor C (thickness t_3) has the most significant influence on the target characteristics with percentage contribution of 38.8397%, followed by factor D (thickness t_4) with percentage contribution of 9.8361%. Factors A (thickness t_1) and B (thickness t_2) have lowest influences. Therefore, factors A and B were pooled into the error.

4.5 Effect of design variables on grey relational grade

A polynomial regression equation for grey relational grade (*GRG*) was constructed using RSM to explain the relationship between the input parameters and the *GRG*. After eliminating the insignificant terms ('Prob > F' larger than 0.05) of parameters, the final mathematic model for *GRG* was precisely achieved. The mathematic models were developed based on the GRG data from 25 experiments. The mathematic model of GRG is developed as follows.

Table 6 Pooled ANOVA for *GRG*

Factors	DOF	SS	V	SS′	P (%)
A	4	Pooled			
B	4	Pooled			
C	4	0.1357	0.0339	0.1112	38.8397
D	4	0.0526	0.0339	0.0282	9.8361
Pooled error	8	0.0979	0.0061	0.2384	51.3242
Total	24				100

Significant at 95% confidence level

$$GRG = 1.7784 - 2.0001t_1 - 1.7772t_2 - 1.1599t_4$$
$$+ 1.2420t_1^2 + 1.7351t_2^2 + 1.2409t_4^2 + .8430t_1t_2$$
$$- 2.5643t_1t_3 + 1.7091t_1t_4 - 2.2124t_2t_4 \quad (25)$$

The two-dimensional contour plots were carried out to demonstrate the effect of controlling factors on *GRG*. The grey relational grey could be predicted based on the various colors. As seen in Figs. 12, 13, 14 and 15, *GRG* is less than 0.4 corresponding to white color contours. *GRG* gradually increases along with more bold green color areas. *GRG* is more than 0.7 corresponding to most bold green color areas. The larger *GRG* is, the better quality characteristics are.

4.6 Developed model adequacy and fitness test

ANOVA was used to check the statistical adequacy of the developed mathematical models Eqs. (23), (24), and (26) On the other hand, ANOVA was utilized to determine the significance of the coefficients and the fitness of the developed models. Based on results of ANOVA, F-value and *p* value are conducted to test the adequacy of developed mathematic models, including displacement, frequency, and *GRG* models. The significance of model terms is proved when the computed F-value is higher than critical F-value tabulated from the standard table at 95% confidence level (Phillip 1996), and 'Prob > F' (p-value) is less than 0.05. The fitness of model is tested based on the determination coefficient (R-squared value) and R-squared (adjusted) (Dao and Huang 2015) to test whether the data are well fitted in the model or not.

Fig. 12 Contour plot of GRG versus t_1 and t_2
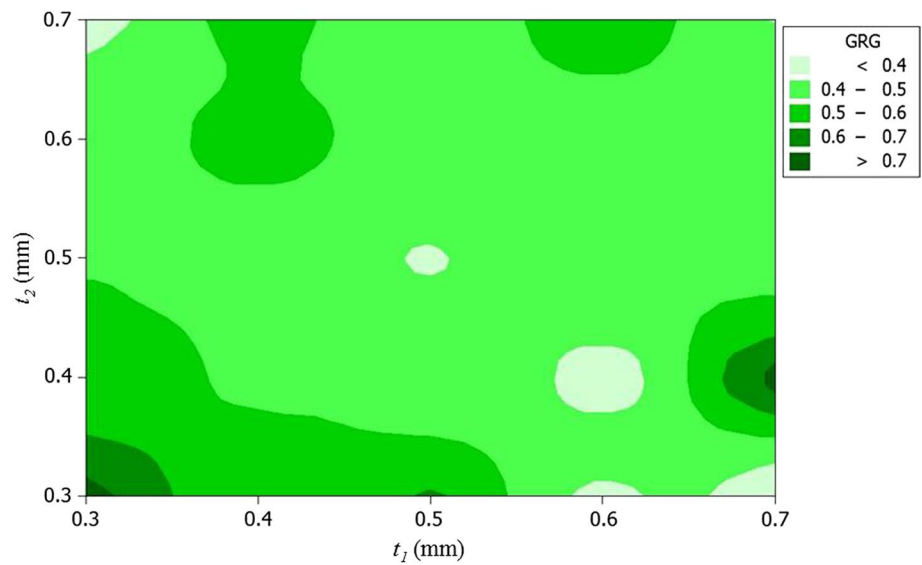
Fig. 13 Contour plot of GRG versus t_1 and t_3
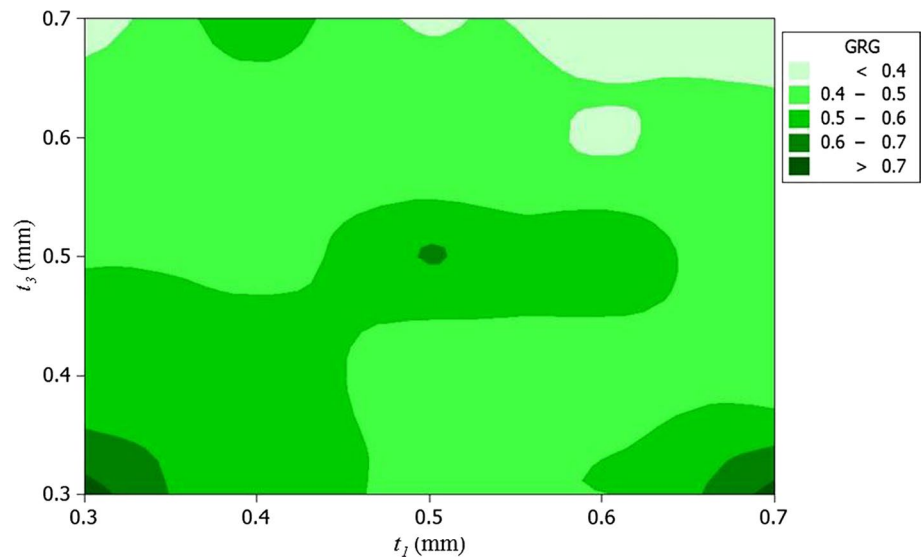
By using regression method, the insignificant model terms were eliminated. The ANOVA results for the reduced quadratic models were given in Tables 7, 8, and 9, which illustrate the significant model terms. The results of ANOVA in Tables 7, 8, and 9 indicated that the F-value of the models which proves their significances because computed F-value of the model terms is all higher than the critical F-value tabulated from the standard table at 95% confidence level (Phillip 1996). The results found that p-value of source of the regression models and coefficients were less than 0.007. ANOVA results revealed that the developed models for the models (y_1, y_2, and GRG) are significant and adequate. The R-squared value for three models is close to utility in Tables 7, 8, and 9. It represents an excellent fitness of experimental data to the developed mathematic models.

4.7 Accuracy validation of developed model

ANOVA was first used to test the adequacy and fitness of the developed models. And then, the prediction accuracy and adequacy of the developed models were confirmed using the experimental investigation. The parameters t_1 of 0.36 mm, t_2 of 0.43 mm t_3 of 0.50 mm, and t_4 of 0.65 mm were selected randomly in their ranges to manufacture four prototypes. These parameter levels were substituted into Eqs. (23), (24), and (25) to achieve the mean predicted value for each mathematic model. Next, prototype was manufactured and each validation experiment was conducted four times to get the mean actual value for each model. Subsequently, the predicted results were compared with the actual results to validate prediction accuracy of the developed models. The results of Table 10 indicated that the deviation errors between

Fig. 14 Contour plot of GRG versus t_1 and t_4
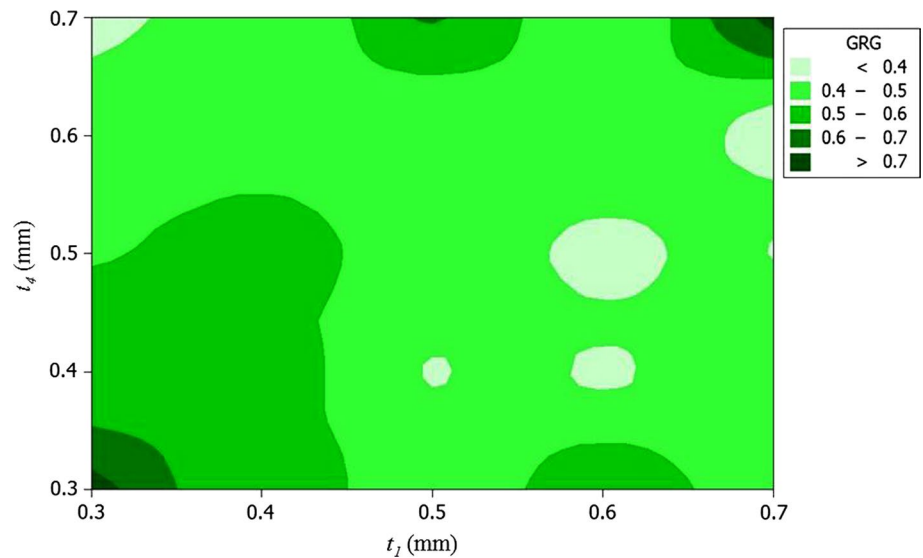
Fig. 15 Contour plot of GRG versus t_2 and t_4
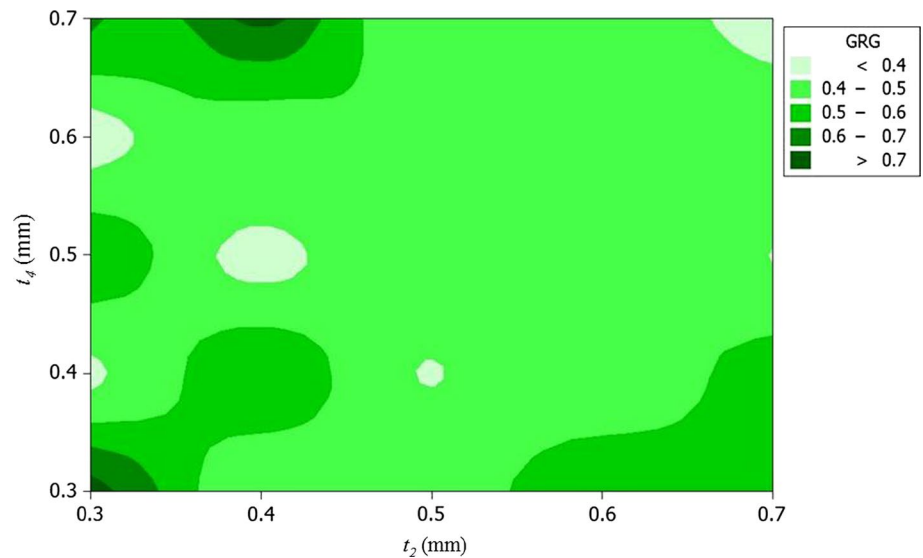
Table 7 ANOVA result for response surface model of displacement

Source	DOF	F-value	p-Value	Remark
Regression	10	247.47	0.000	Significant
Linear	4	67.82	0.000	Significant
t_1	1	57.70	0.000	Significant
t_2	1	16.81	0.001	Significant
t_3	1	93.53	0.000	Significant
Interaction	6	21.32	0.000	Significant
$t_1 \times t_2$	1	12.08	0.004	Significant
$t_1 \times t_3$	1	29.58	0.000	Significant
$t_2 \times t_3$	1	28.65	0.000	Significant
Residual error	14			
Total	24			

R-Squared = 99.44%, R-Squared (adjusted) = 99.04%

Table 8 ANOVA result for response surface model of frequency

Source	DOF	F-value	p-Value	Remark
Regression	10	23.66	0.000	Significant
Interaction	6	33.30	0.000	Significant
$t_1 \times t_2$	1	11.04	0.005	Significant
$t_1 \times t_3$	1	16.00	0.001	Significant
$t_1 \times t_4$	1	10.55	0.006	Significant
$t_2 \times t_4$	1	89.18	0.000	Significant
Residual error	14			
Total	24			

R-Squared = 94.41%, R-Squared (adjusted) = 90.42%

the mean predicted results and the mean actual results are smaller than 5%. These errors revealed that the predictability of the developed mathematic models is accurately reliable.

4.8 Predict the optimal grey relational grade under optimum parameters

In this study, the optimal grey relational grade is predicted considering the effect of all controlling parameters at optimal level A1B1C1D1. The estimated mean of the grey relational grade is determined by Eq. (21), and then 95% confidence interval of confirmation experiments (CI) is calculated using Eq. (22). The expected mean value of four confirmation experiments was obtained as follows.

$\mu_G = 0.7517, F_{0.05}(1, 8) = 5.3177$, $V_e = 0.0061$(get from Table 7), $n_{eff} = 25/(1 + 16) = 1.4705$, $Re = 4$, CI $= \pm 0.1737$.

Table 9 ANOVA result for response surface model of *GRG*

Source	DOF	F-value	p-Value	Remark
Regression	12	51.02	0.000	Significant
Linear	4	19.13	0.000	Significant
t_1	1	36.62	0.000	Significant
t_2	1	19.02	0.001	Significant
t_4	1	10.56	0.007	Significant
Square	4	22.68	0.000	Significant
$t_1 \times t_1$	1	22.61	0.000	Significant
$t_2 \times t_2$	1	29.55	0.000	Significant
$t_4 \times t_4$	1	15.12	0.002	Significant
Interaction	4	42.81	0.000	Significant
$t_1 \times t_2$	1	32.00	0.000	Significant
$t_1 \times t_3$	1	42.49	0.000	Significant
$t_1 \times t_4$	1	27.52	0.000	Significant
$t_2 \times t_4$	1	82.70	0.000	Significant
Residual error	12			
Total	24			

R-Squared $= 98.08\%$, R-Squared (adjusted) $= 96.16\%$

Table 10 Comparison between predicted and actual responses

Model	Mean predicted value	Mean actual value	Error (%)
y_1 (mm)	0.109	0.114	3.96
y_2 (Hz)	904.081	912.846	1.00
GRG	0.5910	0.5780	2.24

$$0.5780 \le \mu_{confirmation} \le 0.9254 \qquad (26)$$

4.9 Confirmation experiments

By using optimal combination A1B1C1D1, which the optimal values of design parameters were as follows: $t_1 = 0.3$ mm, $t_2 = 0.3$ mm, $t_3 = 0.3$ mm, $t_4 = 0.3$ mm, four confirmation experiments were performed to validate the optimal results. The experimental results of Table 11 revealed that the confirmation GRG results fall within 95% of the CI. The deviation errors between the predicted optimal values and confirmation optimal values were approximately less than 3%. Consequently, it is clearly proved that the quality characteristics of TDCM can be efficient improved by using the hybrid approach of grey-Taguchi based response surface methodology and entropy measurement technique. Four models were constructed in Solidworks and then by a finite element method (FEM) ANSYS 13 was used to validate the optimal results. The automatic method was applied for meshing the model of the compliant stage, as shown in Fig. 16. The 10-node tetrahedral structural solid element of the SOLID 92 type was adopted for meshing the model. The flexure hinges were refined to achieve the better accurate results. The results showed that the errors between FEM result and predicted value are less than 5%, as seen in Table 11. It means that the optimal setting of design variables can be predicted well by the proposed hybrid approach.

5 Conclusions

This study has attempted to multi-objective optimal design for TDCM based on statistical techniques as Taguchi, response surface methodology, grey relational analysis and entropy weighting measurement technique. The various thickness of flexure hinges were chosen to be design variables because it affected to the quality characteristics such as the displacement and the first natural frequency of TDCM. The experimental plan was conducted by the Taguchi's L_{25} orthogonal array to save time and costs.

A hybrid approach of grey-Taguchi based response surface methodology and entropy measurement was coupled to multi-response optimal process to overcome the disadvantages of the Taguchi method in multiple quality analysis. Response

Table 11 Predicted and confirmation values

Response	Optimum parameters	Predicted value	Actual value	FEM value	Error %	
					FEM and predicted values (%)	Actual and predicted values (%)
Displacement (mm)	A1B1C1D1	0.167	0.171	0.175	4.79	2.05
Frequency (Hz)		902.597	909.638	912.103	1.05	1.39
GRG		0.7517	0.6097	0.7162	4.72	2.95
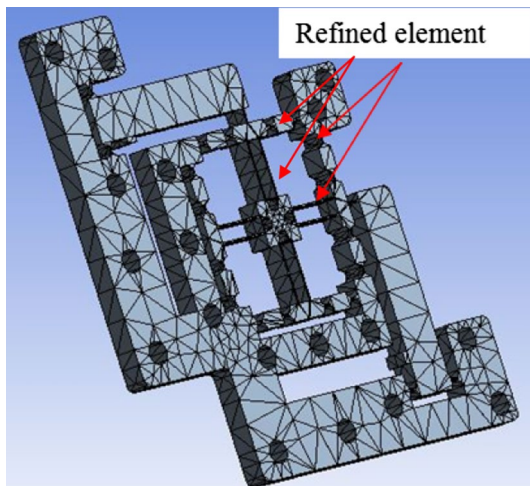
Fig. 16 Meshed model of TDCM

surface methodology was used for modeling the relationship between design variables and two responses as well as the relationship between design variables and the grey relational grade. Entropy weighting quality measurement technique was applied for calculating the weight factor corresponding to each of quality characteristics. ANOVA was performed to determine the significant contributions of parameters affecting the *GRG*. ANOVA and confirmation tests were then conducted to validate the prediction accuracy and the statistical adequacy of the developed mathematical models.

The optimal combination of design variables were determined based on the main effect analysis. The optimal performances of TDCM were also obtained. The experimental results were in a good agreement with the simulation results from ANSYS. It hopes that the proposed methodology can be widely used for related compliant mechanisms.

References

Chiang YM, Hsieh HH (2009) The use of the Taguchi method with grey relational analysis to optimize the thin-film sputtering process with multiple quality characteristic in color filter manufacturing. Comput Ind Eng 56:648–661. doi:10.1016/j.cie.2007.12.020

Dao TP, Huang SC (2016) Design and analysis of a compliant micropositioning platform with embedded strain gauges and viscoelastic damper. Microsyst Technol 1–16. doi:10.1007/s00542-016-3048-3

Dao TP (2016) Multiresponse optimization of a compliant guiding mechanism using hybrid t-grey based fuzzy logic approach. Math Probl Eng 2016:1–17. doi:10.1155/2016/5386893

Dao TP, Huang SC (2015) Robust design for a flexible bearing with 1-dof translation using the Taguchi method and the

utility concept. J Mech Sci Technol 29:3309–3320. doi:10.1007/s12206-015-0728-3

Datta S, Nandi G, Bandyopadhyay A (2009) Application of entropy measurement technique in grey based Taguchi method for solution of correlated multiple response optimization problems: a case study in welding. J Manuf Syst 28:55–63. doi:10.1016/j.jmsy.2009.08.001

Ilo S, Just C, Xhiku F (2012) Optimisation of multiple quality characteristics of hardfacing using grey-based Taguchi method. Mater Des 33:459–468. doi:10.1016/j.matdes.2011.04.050

Kuo CFJ, Su TL, Jhang PR, Huang CY, Chiu CH (2011) Using the Taguchi method and grey relational analysis to optimize the flat-plate collector process with multiple quality characteristics in solar energy collector manufacturing. Energy 36:3554–3562. doi:10.1016/j.energy.2011.03.065

Li Y, Xu Q (2011) A novel piezoactuated XY stage with parallel, and stacked flexure structure for micro-/nanopositioning. IEEE Trans Ind Electron 58:3601–3615. doi:10.1109/TIE.2010.2084972

Montgomery DC (1997) Design and analysis of experiments. Wiley, New York

Muthuramalingam T, Mohan B (2014) Application of Taguchi-grey multi responses optimization on process parameters in electro erosion. Measurement 58:495–502. doi:10.1016/j.measurement.2014.09.029

Phillip R (1996) Taguchi techniques for quality engineering. MCGraw-Hill, New York

Senthilkumar N, Tamizharasan T, Anandakrishnan V (2014) Experimental investigation and performance analysis of cemented carbide inserts of different geometries using Taguchi based grey relational analysis. Measurement 58:520–536. doi:10.1016/j.measurement.2014.09.025

Sharma A, Yadava V (2012) Modelling and optimization of cut quality during pulsed Nd:YAG laser cutting of thin Al-alloy sheet for straight profile. Opt Laser Technol 44:159–168. doi:10.1016/j.optlastec.2011.06.012

Wang PY, Xu Q (2017) Design of a flexure-based constant-force XY precision positioning stage. Mech Mach Theory 108:1–13. doi:10.1016/j.mechmachtheory.2016.10.007

Wen KL, Ting CC, Mei LY (1998) The grey entropy and its application in weighting analysis. IEEE Int Conf Syst Man Cybern 2:1842–1844. doi:10.1109/ICSMC.1998.728163

Xu Q (2012a) New flexure parallel-kinematic micropositioning system with large workspace. IEEE Trans Robot 28(2):478–491. doi:10.1109/TRO.2011.2173853

Xu Q (2012b) Design and development of a flexure-based dual-stage nanopositioning system with minimum interference behavior. IEEE Trans Autom Sci Eng 9(3):554–563. doi:10.1109/TASE.2012.2198918

Xu Q (2012c) Mechanism design and analysis of a novel 2-dof compliant modular microgripper. In: 7th IEEE conference on industrial electronics and applications (ICIEA), 1966–1971. doi:10.1109/ICIEA.2012.6361051

Xu Q (2014) Design and development of a compact flexure-based xy precision positioning system with centimeter range. IEEE Trans Ind Electron 61(2):893–903. doi:10.1109/TIE.2013.2257139

Xu Q (2016) Design and implementation of large-range compliant micropositioning systems. Wiley, New York. doi:10.1002/9781119131441

Yong YK, Lu TF, Handley DC (2008) Review of circular flexure hinge design equations and derivation of empirical formulations. Precis Eng 3:63–70. doi:10.1016/j.precisioneng.2007.05.002

Zhang X, Zhang Y, Xu Q (2016) Design and control of a novel piezodriven XY parallel nanopositioning stage. Microsyst Technol 1–14. doi:10.1007/s00542-016-2854-y